Engineering Failure Analysis 151 (2023) 107354

Contents lists available at ScienceDirect

Engineering Failure Analysis

journal homepage: www.elsevier.com/locate/engfailanal

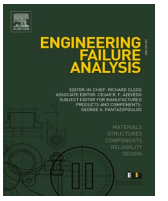

Failure analysis and structural reliability of unreinforced masonry veneer walls: Influence of wall tie corrosion

Imrose B. Muhit [a,*], Mark J. Masia [b], Mark G. Stewart [c]

[a] School of Computing, Engineering and Digital Technologies, Teesside University, Tees Valley TS1 3BX, United Kingdom
[b] Centre for Infrastructure Performance and Reliability, The University of Newcastle, Callaghan, NSW 2308, Australia
[c] School of Civil and Environmental Engineering, University of Technology Sydney, Ultimo, NSW 2007, Australia

ARTICLE INFO

Keywords:
Corrosion
Historical
Masonry
Veneer wall
Wall tie
Spatial variability
Structural reliability

ABSTRACT

Corrosion appears to be a very common problem in historical and aged structures with steel ties and anchorages. A potential rapid deterioration of the wall tie due to the corrosion leading to a premature structural failure poses a serious threat to the built heritage infrastructures' safety. This paper describes an overview of the probabilistic failure analysis of the unreinforced masonry (URM) veneer wall system with flexible backup under uniformly distributed out-of-plane loadings. Moreover, a framework is proposed to consider the wall tie corrosion in the stochastic finite element analysis (FEA) while estimating the structural reliability. A probabilistic experimental study where 18 full-scale URM veneer wall systems with theoretically identical geometries and properties were tested under inward and outward lateral loading. Wall failure statistics along with the probabilistic characterisation of veneer wall constituent materials including mortar, wall tie and timber were accomplished. A stochastic computational model was then developed which combines the FEA and Monte Carlo simulation to evaluate the failure progression and system peak load (veneer capacity) while considering the spatial variability of veneer wall material properties. Two scenarios, with and without wall tie corrosion, are considered, and the probabilistic characterisation of the veneer capacities for these scenarios under inward and outward out-of-plane loading is also reported. The model error statistics were combined with the probabilistic load models to determine the reliability index corresponding to the Australian Standard for Masonry Structures AS 3700. Annual reliabilities are compared to target reliabilities recommended by ISO 2394. Capacity reduction factor and design minimum tie strength consideration for corroded wall tie is also discussed.

1. Introduction

Unreinforced masonry (URM) is mostly used as structural components in low-rise apartments, townhouses and single-dwelling houses and as facades in low-rise and multi-storey framed buildings. Generally, a masonry veneer wall is an external wythe of masonry connected to a backup system with different types of ties and the backup systems range from non-loadbearing enclosure walls in reinforced concrete frames, through structural masonry or concrete walls, to light timber and steel stud frames [1]. In Australia and New Zealand, timber is widely used as a flexible backup system (see Fig. 1). Ties play a significant role in the performance of brick

* Corresponding author.
E-mail addresses: i.muhit@tees.ac.uk (I.B. Muhit), mark.masia@newcastle.edu.au (M.J. Masia), mark.stewart@uts.edu.au (M.G. Stewart).

https://doi.org/10.1016/j.engfailanal.2023.107354
Received 9 March 2023; Received in revised form 4 May 2023; Accepted 21 May 2023
Available online 7 June 2023

veneers as they are intended to ensure the masonry panels' lateral stability. Hence the inadequate structural performance of ageing and contemporary masonry veneer wall is mostly due to the lack of ties, larger spacing than the one recommended by codes and/or deteriorated or corroded ties.

The first use of wall ties, such as wrought iron ties, inside cavity walls, appears to have been in England in the mid-1800 s [2]. With the increasing use of masonry construction, many different metal wall-tie systems began to be developed in the early 1960 s [2]. For the historical or ageing masonry structure along with the ageing of an entire masonry system, corrosion of wall ties (see Fig. 2) is a significant problem that often is not observed until it is too late. In extreme cases, wall tie deterioration is only apparent after the collapse of the outer leaf of the masonry, just as occurred as a result of the Newcastle Earthquake in 1989, in which a 5.6 strength earthquake on the Richter scale damaged 3,000 buildings, killed 13 people and cost over $4 billion [3]. Extensive research after the earthquake revealed the corrosion of wall ties was a major cause of the loss of stability of masonry leaves and the consequent failure of masonry walls [4]. Moreover, following the devastating Hawke's Bay earthquake (New Zealand) in 1931, Dowrick [5] reported that many non-residential URM buildings were severely damaged after being subjected to strong ground shaking. As a consequence, the use of unreinforced masonry in New Zealand construction, including cavity walls, declined dramatically due to their observed inadequate seismic performance. In 2017, part of a three-storey brick wall collapsed from an 88-year-old building in Western Australia also as a consequence of severe weather and windstorms. Moreover, medieval and masonry bell towers are highly vulnerable to seismic failure and seismic assessment of such structures is reported by Preciado et al. [6]. The risk of collapse and structural safety concerns of built heritage structures due to corrosion of wall ties is widely documented in the literature [7 –12] and the International Scientific Committee for the Analysis and Restoration of Structures of Architectural Heritage (ISCARSAH) recommendations [13].

Due to the lack of information, the actual level of safety of historical and ageing masonry structures is not known. Apart from the random corrosion of wall ties the problem is further compounded by the fact that the strength properties of masonry are highly variable, particularly the unit-to-unit flexural bond strength, due to variations in the quality of workmanship, the weather during construction, the difficulty of controlling site-batched mortar and the materials from location to location, all within one structure [14]. However, most of the existing analyses [15–18] of veneer wall systems assume homogenous material properties for flexural bond strength in the masonry wall, rather than considering the unit-to-unit spatial variability of flexural bond strength, the latter being a more realistic approach in examining material variability. Variations of material properties can be incorporated into a numerical modelling study and the most popular method of realising this kind of modelling work is finite element analysis (FEA) combined with Monte-Carlo simulation (MCS). Li et al. [19] developed the stochastic computational model combining the FEA and MCS for single-leaf brick masonry walls under uniform pressure loads. On the other hand, Muhit et al. [20] developed the spatial stochastic FEA model of veneer wall system components (masonry, wall tie and timber) subjected to one-way vertical bending and compared it with test results of 18 full-scale veneer walls under inward and outward lateral out-of-plane loading [21].

While other international codes have revised and adjusted their factor of safety in order to improve reliability, the load capacity reduction factor (ϕ) of the Australian masonry standards AS 3700 [22] remains mostly unchanged since the 1980 s. Several approaches [23 –25] to calibrating the ϕ for one-way bending in AS 3700 [22] have been considered. To calculate the service life of wall ties Drysdale [26] proposed a general guide for the service life of zinc for various environments and evaluate the sacrificial rate of zinc loss in accordance with ASTM A153 [27]. Nevertheless, none of these studies considered the veneer or cavity wall systems with

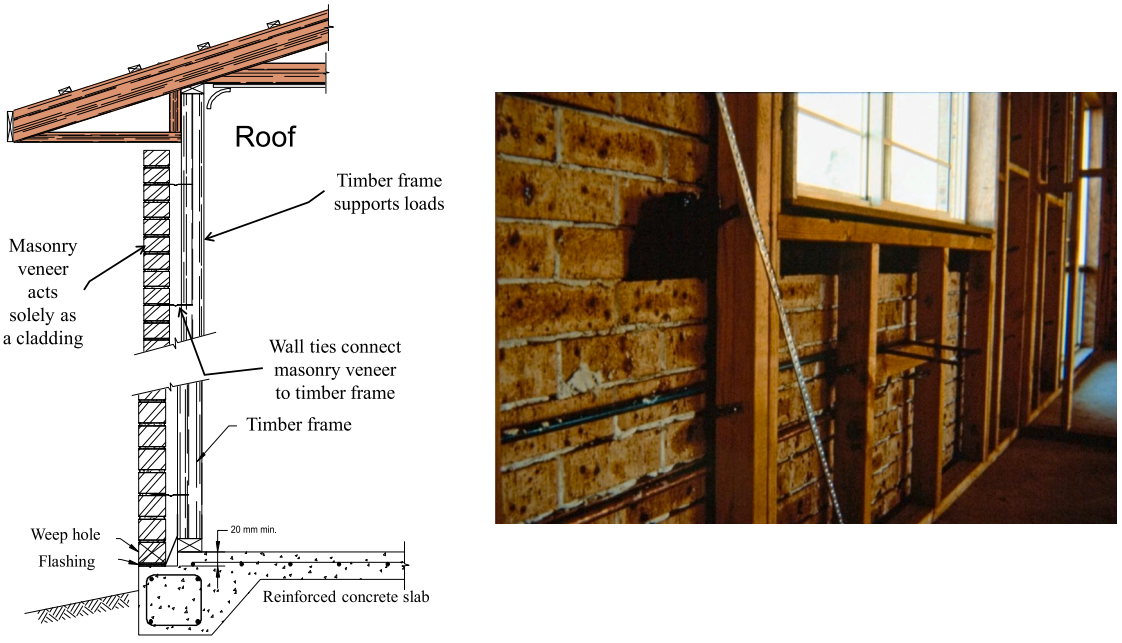

Fig. 1. Masonry veneer wall details with flexible backup system (Think Brick Australia).

Fig. 2. Corrosion of the part of the tie embedded in mortar (Photograph taken by Prof. Adrian Page in 1989 the after Newcastle Earthquake).

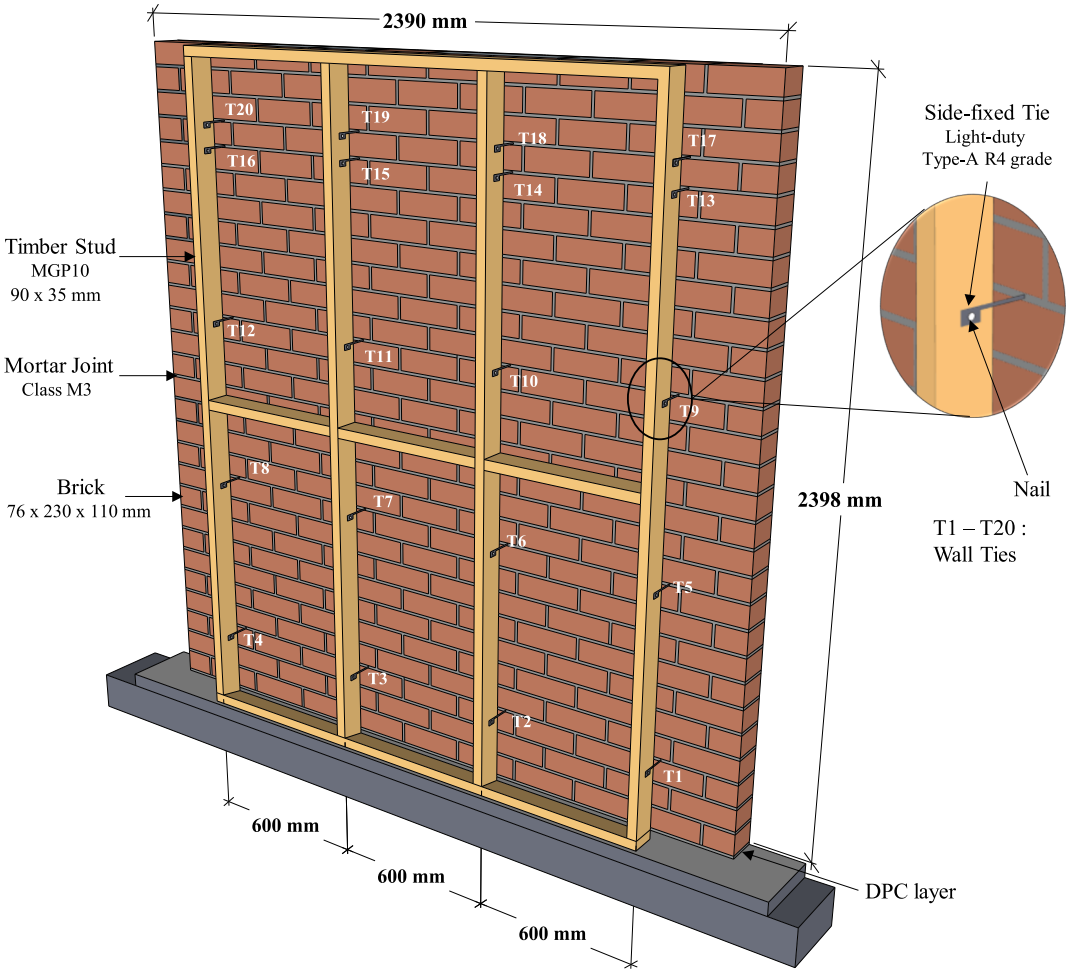

Fig. 3. Elevation of the full-sized URM veneer wall system [21].

deteriorated or corroded wall ties to estimate the failure load where unit-to-unit spatial variability of the wall constituent materials is considered. Moreover, computational model(s) or framework for reliability-based assessment of masonry veneer walls under the influence of corrosion is absent from the literature.

(a)

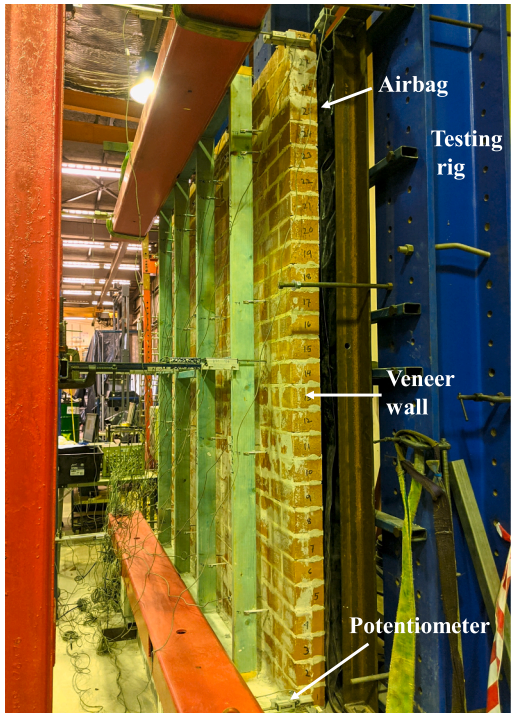

(b)

Fig. 4. Veneer wall testing for (a) inward and (b) outward loading in the laboratory [21].

In this paper, a research framework is established to assess the structural reliability of the unreinforced masonry veneer wall system subjected to uniform out-of-plane loading (i.e., wind loading) considering the influence of corroded wall ties. To develop this framework, a large-scale laboratory testing programme along with probabilistic material characterisations were carried out. Then stochastic models combining finite element analysis and Monte-Carlo simulation (MCS) account for spatial variability of the veneer wall constituent materials when estimating the veneer capacity. The effect of corrosion of ties is considered by reducing wall tie strength in the veneer walls and compared with non-corroded ties (i.e., new construction). Model error statistics are then combined with the results of the spatial stochastic FEA and probabilistic load models to determine the reliability index corresponding to the AS 3700 [22] design of veneer walls with flexible structural backing. Changes in the capacity reduction factor and minimum tie strength required to meet the target reliability index are also discussed. The developed framework can be applied to evaluate the safety and understand the failure mechanism of architectural heritage structures with wall ties and steel anchorages subjected to extreme events like wind loading.

2. Monte-Carlo laboratory testing of URM veneer wall system

2.1. Full-scale experimental programme

To improve the current design practice and evaluate the structural reliability of the veneer wall system, it is imperative to conduct full-scale testing of masonry veneer and facade systems, including multiple repeat specimens to deduce probabilistic distributions of collapse loads. Hence, Monte-Carlo laboratory testing was accomplished for 18 masonry veneer assemblies of theoretically identical properties (geometry, type of masonry, wall ties, stress grade of timber stud, etc.) under inward and outward loading. Among these identical 18 veneer walls, ten walls were tested in compression (inward loading on the wall surface and ties are in compression) and eight in tension (outward loading and ties are in tension) by means of lateral pressure loading. The dimension of the wall assembly was 2398 mm (height) × 2390 mm (length) × 110 mm (thickness) with 10 mm fully bedded mortar joints (mixing ratio of 1:1:6 for cement: lime: sand by volume), as shown in Fig. 3. These adopted dimensions allow four vertical lines of ties spaced at a maximum spacing of 600 mm as per AS 3700 [22], and plausibly a higher chance of a weak mortar joint to initiate cracking due to additional joints across the length of the wall, in contrast to a shorter wall. To transfer face loads from a veneer to a structural backing, a light-duty 'Type A' (non-seismic areas) veneer tie with durability classification R4 (stainless steel grade) was used in this experimental program. Each wall tie is 8.25 mm^2 in cross-sectional area and side fixed from masonry wall to timber studs with 50 mm cavity width (clear distance between the masonry leaf and timber studs). Machine-graded pine with stress-grade MGP10 timber studs (90 mm × 35 mm in cross-section) were used as a flexible structural backup and are chosen as per standard requirements for timber-framed residential housing. The wall consists of a single leaf of a masonry wall and another leaf of timber studs, connected in between with five rows of ties including double rows of ties at the top as per AS 3700 [22] requirement for the single-storey veneer. Each wall (mortar) was cured for a minimum of 14 days, and ties were nail fastened with timber studs prior to wall testing.

Two inflatable airbags positioned within a closed loading frame simulated the uniform wind pressure (evenly distributed lateral out-of-plane loading) on the masonry veneer. For the monotonic testing, the pressure was applied through compressed air and gradually increased until the post-peak lateral pressure dropped by at least 20% of the peak load or failure (collapse) of the specimen. One wall specimen from each category (inward and outward loading) was tested under the semi-cyclic loading, where the pressure load was increased in increments of 0.5 kPa and unloaded to approximately zero each time. For the inward loading case (i.e., ties are in compression), monotonic (for nine wall specimens) and semi-cyclic (for one wall specimen) lateral load was applied directly to the outer leaf of the masonry through the airbag system (see Fig. 4(a)). On the other hand, polystyrene blocks were placed between the airbag and the veneer wall (see Fig. 4(b)) to transfer airbag pressure to the veneer without touching the timber stud frame as the outward loading setup intends that the veneer wall system would experience suction type loading. The entire wall was instrumented with linear variable differential transformers (LVDTs) in a way that the movement of all wall ties across the cavity, in and out-of-plane movement of the masonry wall at different heights, and timber deflections can be captured. For measuring the tie displacement across the air cavity (between the masonry wall and timber stud), an LVDT was mounted beside every tie. Four LVDTs were located on the masonry wall at the mid-height to determine the mid-height deflection of the masonry wall. For inward loading, four LVDTs were installed at the mid-height level of all four timber studs while for outward loading two LVDTs were placed on two extremities of the wall to capture the displacement history of the outer two timber studs. A total of 38 LVDTs for inward loading and 31 LVDTs for outward loading were used to monitor and measure all displacements throughout the veneer wall system. All LVDTs used had a 50 mm stroke length (0.1% linearity) except for mid-height level LVDTs which are 100 mm in length (0.1% linearity). The reader is referred to Muhit et al. [21] for the details of support conditions and the instrumentation arrangement for the inward and outward loading tests. The wall specimens for inward and outward loading were labelled as Veneer Wall Inward, VWI_<Test repeat > and Veneer Wall Outward, VWO_<Test repeat>, respectively.

2.2. Probabilistic material characterisations

2.2.1. Masonry characterisation and flexural bond strength statistics

The mechanical properties of the masonry materials were obtained in accordance with standard test methods, as follows: flexural tensile strength of the brick [28], flexural tensile strength of the mortar joint [22], mortar joint cohesion and friction [29], and masonry compressive strength and elastic modulus [22].

Each veneer wall specimen was constructed using two batches of mortar (MB-I and MB-II). For each batch of mortar mixed, two ×

six-unit high masonry piers were constructed for bond wrench testing (to determine the flexural tensile strength of the mortar joints, f_{mt}) at the same age as the associated wall constructed using that mortar. As the measured mechanical properties (flexural tensile strength) are not precisely the same for both batches for the same wall, it is crucial to assess whether batch-to-batch variabilities, i.e., between or within batches, are significant or not. To determine if two data sets of two mortar batches came from the same population, the student's *t*-test (inferential statistical hypothesis test) was applied and the outcome indicated that for most of the wall specimens, the two mortar batches can be considered from the same population. This outcome is expected because both mortar batches were prepared in an identical controlled environment, at roughly the same time, and materials are sourced from the same supplier. Table 1 shows the statistical comparison between batches (aggregated) for inward and outward-loading specimens. This also confirms that between batch variability is low. Based on the findings from the batch-to-batch variability studies, MB-I and MB-II data sets were aggregated, and a range of probability distributions were fitted to all bond strength data points of VWI and VWO samples using the maximum likelihood method. The Anderson-Darling (A-D) test at the 5% significance level was performed to check the goodness-of-fit to the lower tail of the distribution as this has more influence to wall failure progression compared to the whole distribution. For both loading types, The A-D test could not reject the lognormal distribution and ranked it highest among the available hypothesised distributions; hence, considered as the best fit.

2.2.2. Masonry veneer wall tie characterisation

The mechanical properties of steel, by which the tie is made of, are not highly variable like masonry; however, when these steel anchorages are incorporated with mortar and timber their strengths and stiffnesses are no longer constant for all ties in a masonry veneer wall system. This might be due to the manual installation of wall ties, the variability of flexural bond strength of mortar joint and the immense variability in mechanical properties of timber [30] make the brick-tie-timber assembly highly variable. Moreover, the testing of brick-tie-timber subassemblies (the couplet) is more realistic and rational than testing the ties in isolation to characterise the local behaviour of a wall system. Therefore, an extensive 'Monte-Carlo experimental study' of the couplet under axial compression and tension loading, considering one of the leaves (brick) is fixed and the relative motion of the free leaf (timber) occurs in the perpendicular direction (axial loading of the tie) is accomplished and details of this study can be found at Muhit et al. [31]. The couplets were constructed with two standard perforated clay bricks (230 mm long × 110 mm wide × 76 mm high), one timber stud (150 mm in length and 90 mm × 35 mm in cross-section), and one corrugated tie. The type of tie, timber and mortar mixing ratio is kept identical to full-scale wall tests. A total of 50 couplet specimens were tested using a displacement control Instron electromechanical testing system, 25 under compression and 25 under tension loading. For compression tests, almost all (23 specimens) specimens failed by axial buckling of the tie, and only two specimens failed by the combination of tie buckling and pull-out of the nail from timber. On the contrary, ductile nail pull-out from the timber stud was observed for all specimens under tension loading. It's worth noting that, the failure mechanism of corroded tie couplet may be influenced by the level and position of corrosion and eventually induce higher variabilities. For the corroded wall ties under compression loading, different failure mechanisms than that reported here (axial buckling) may not be expected; nevertheless, pull-out of the tie from the mortar joint, tie hole yielding and/or tie rupture may potentially be observed for the tension scenarios.

All load–displacement curves and a multilinear mean ideal curve (generated based on the average of all actual load–displacement relationships) for compression specimens and tension specimens are shown in Fig. 5. The points/zones selected for the idealised curve are based on the assumption to capture the load–displacement behaviour as accurately as possible. For the compression scenario, after buckling, the load was decreased significantly up to 7 mm displacement, followed by load fluctuations to a lesser extent. The mean buckling load and corresponding displacement were 1.04 kN and 3.08 mm, respectively. For tension, the variation of peak load and the post-peak behaviours are notably higher compared to the compression behaviour due to the variable nature of the nail pull-out failure. The mean peak load and associated displacement were calculated as 1.32 kN and 7.36 mm, respectively.

As the idealised curves are generated based on the mean values of 25 data points for each defining point (e.g., A, B.., etc.), each point has an individual mean, COV and distribution. Moreover, both the peak loads (failure load) and corresponding displacements are variable at the same time, which means point B (for compression) and point C (for tension) should be defined with the multivariate distribution. Using the maximum likelihood method, a range of probability distributions (Normal, Lognormal, Weibull, Gamma and Gumbel distributions) were fitted to the data sets of all points of idealised curves for compression and tension loading. The Anderson-Darling (A-D) test [32] at the 5% significance level was performed to check the goodness-of-fit. It is a modification of the Kolmogorov-Smirnov (K-S) test [33] and gives more weight to the tails than does the K-S test. Moreover, visual comparisons of inverse cumulative distribution function (CDF^{-1}) plots were executed to infer a goodness-of-fit for the probabilistic models. When CDF^{-1} of a specific probabilistic model sits on the 1:1 line indicates that the model fits well with the data. A summary of statistical parameters of wall tie

Table 1
Statistics of aggregated mortar batches [21].

Specimen Group	Mortar Batch	Data Points	Mean f_{mt} (MPa)	Mean COV	Best-fit Distribution
VWI	MB-I	86	0.40	0.45	–
	MB-II	90	0.39	0.40	–
	Aggregated	176	0.40	0.42	Lognormal
VWO	MB-I	78	0.44	0.45	–
	MB-II	80	0.41	0.49	–
	Aggregated	158	0.42	0.47	Lognormal

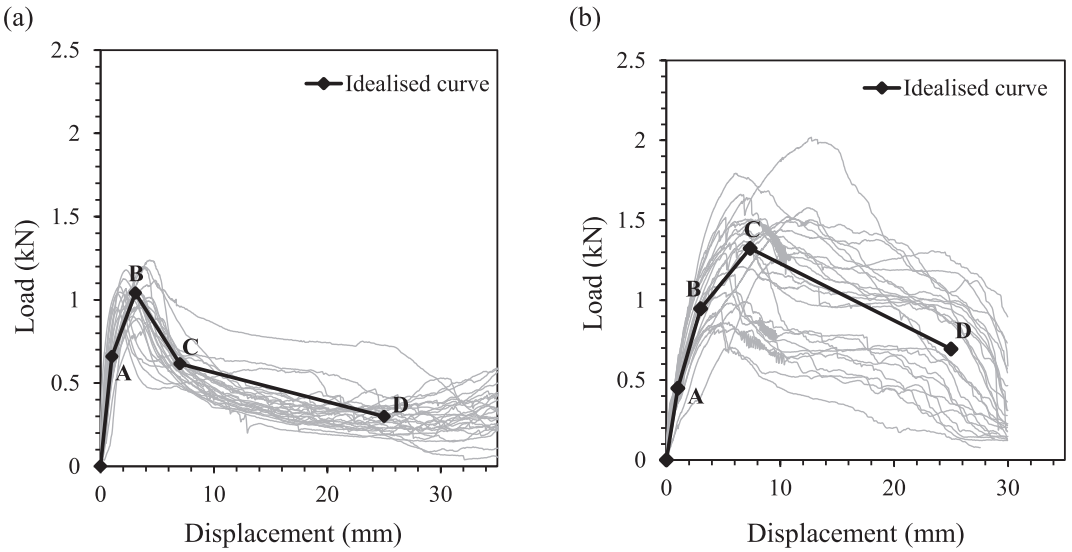

Fig. 5. Load–displacement curves for tie couplet testing with an idealised curve for (a) compression and (b) tension loading.

characterisation is shown in Table 2, where B' and C' represents the displacement at the peak load for compression and tension, respectively.

Pearson's correlation coefficients were calculated for all possible combinations of compression and tension idealised curve along with the peak load and displacement. This correlation coefficient (ρ) has a value between −1 and 1, where zero indicates that there is no linear relation between two variables, positive correlation indicates that a variable rises simultaneously with the other, and the other way around for negative correlation. Based on the findings of this probabilistic tie characterisation, a tie constitutive law is formulated to create a tie material model (see Fig. 6). The first point (point A) of the force–displacement plot for both loadings is a statistically random variable, hence $\rho = 0$.

2.2.3. *Structural timber characterisation*

After the full-scale veneer wall system tests, every timber stud used to construct the veneer wall specimens was tested to evaluate the modulus of elasticity (E) and bending strength (f_b) according to the test method suggested at AS/NZS 4063.1 [34]. A total of 40 and 32 timber studs were tested which were obtained from full-scale veneer wall specimens loaded inward and outward, respectively. For inward and outward loading stud specimens, the respective mean modulus of elasticity was measured as 10275 MPa (COV of 0.18) and 12479 MPa (COV of 0.26). Using the maximum likelihood method, a range of probability distributions were fitted to the stiffness (modulus of elasticity) data sets of all timber specimens and based on goodness-of-fit tests, Gamma and lognormal distributions were found to be the best fit for the inward and outward categories, respectively.

2.3. *Full-scale veneer wall experimental results*

2.3.1. *Inward loading*

During each test, the following observations were recorded: applied pressure, including the wall's load-carrying capacity (wall collapse load), out-of-plane displacements of the masonry veneer, the timber studs and individual tie deformations. Fig. 7(a) shows the mean response (load versus veneer mid-height displacement) for three walls, VWI-1: higher cracking load than any specimens, VWI-2: representative of the remaining eight monotonically tested specimens and VWI-10: subjected to semi-cyclic loading. Each mean

Table 2
Summary of statistical parameters for tie characterization [31].

Sample Type	Data Point	Sample Size	Distribution	Mean Load / Displacement	Unit	COV
Compression	A	25	Normal	0.66	kN	0.28
	B		Lognormal	1.04	kN	0.09
	B'		Normal	3.08	mm	0.35
	C		Lognormal	0.62	kN	0.17
	D		Lognormal	0.30	kN	0.33
Tension	A	25	Normal	0.45	kN	0.24
	B		Normal	0.95	kN	0.22
	C		Normal	1.32	kN	0.23
	C'		Lognormal	7.34	mm	0.32
	D		Normal	0.69	kN	0.49

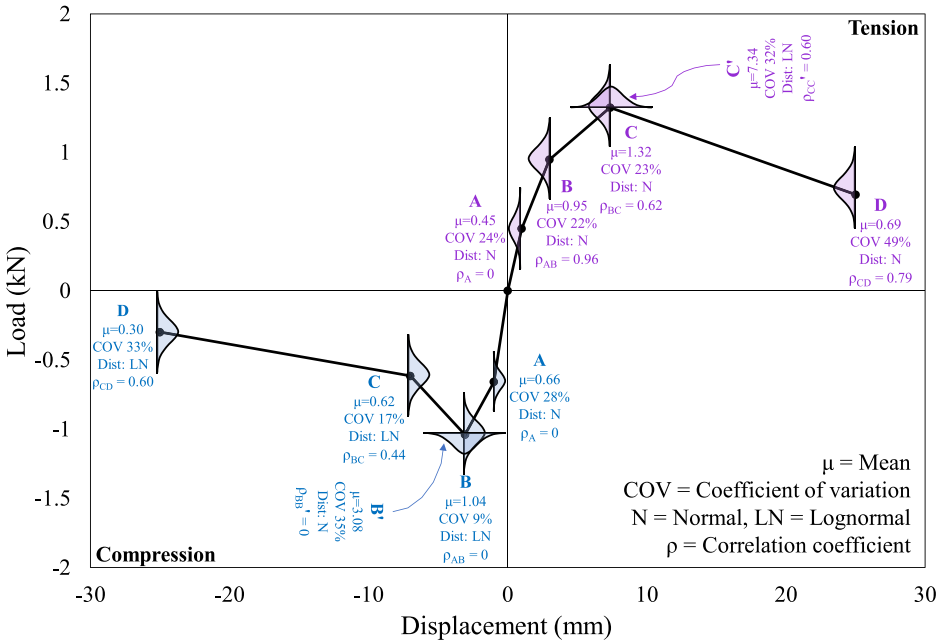

Fig. 6. Summary of tie constitutive law with probabilistic information [31].

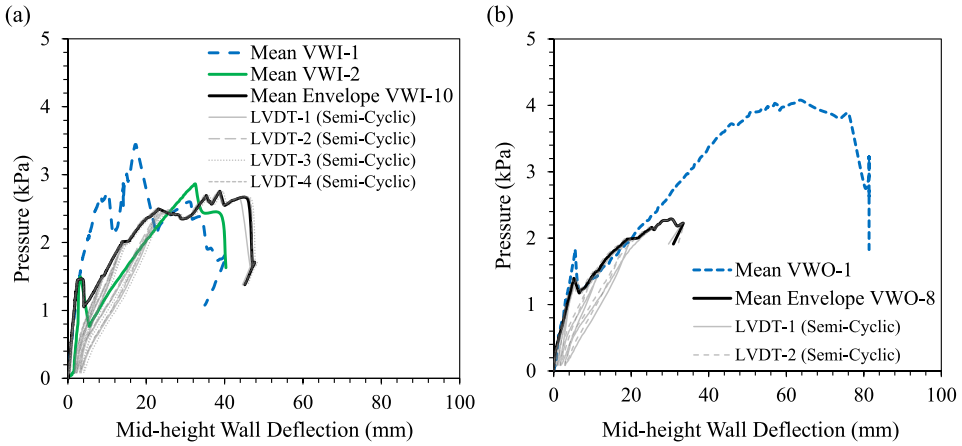

Fig. 7. Pressure vs. mid-height wall deflection of veneer wall specimens under (a) inward and (b) outward loading.

response is the average of four LVDTs installed along the length of the masonry wall at mid-height. Specimen VWI-10 was tested under semi-cyclic loading where the mean-envelope curve was derived to better understand the overall behaviour of this specimen. This mean-envelope curve verifies that the monotonic response envelopes the cyclic response quite closely. The typical trend of the pressure versus wall mid-height displacement curve was, veneer cracking at a mean load of 1.74 kPa (considering VWI-1 as an outlier), followed by a sudden small pressure drop, then increasing pressure until veneer system peak load was achieved at a mean load of 2.80 kPa, where randomly different rows of the wall ties were buckled, or nails pulled out from the timber studs. The COV for the overall veneer system peak load (R_u) was considerably less (0.11) than the COV of masonry cracking load, R_{cr} (0.14), which indicates the higher variability in masonry strength properties compared to other materials (for example, wall ties) in the wall system. Semi-cyclically loaded specimen (VWI-10) showed increased displacement capacity compared to the monotonically tested specimens (38.78 mm for VWI-10 compared to mean 27.13 mm). This behaviour might be due to the repetitive loading–unloading pattern, i.e. when the wall specimen is unloaded, there is a residual displacement for each cycle (see Fig. 7(a)) which helps the wall to deflect further.

Masonry veneer cracking initiates when flexural tensile stresses normal to the bed joints exceed the flexural tensile strength (bond strength) of the masonry. The exact location of cracking would depend upon the maximum flexural tensile stress induced by the applied out-of-plane pressure loading and the presence of a weak joint (low bond strength) and the level of precompression on the joint due to the wall self-weight. Therefore, spatial variability in masonry joint strengths plays a significant role in defining the location of

veneer cracking. During wall tests, eight out of ten walls exhibited a single horizontal layer of the crack through the brick–mortar interface and statistically, there is an 80% probability of having cracks in brick courses nearest to the second rows of wall ties (courses 10–11 to 14–15). In terms of tie failures, four types of tie failure modes were observed from wall system testing, typical buckling (at 90°) at the cavity, folding inside or near the tie-mortar joint, a combination of buckling at the cavity and folding inside the mortar joint, and tie connection (nail) pull-out from the timber stud.

2.3.2. Outward loading

The pressure vs. mid-height veneer displacement behaviours for the two representative veneer wall outward loading tests (one from monotonic, VWO-1, and one from semi-cyclic loading, VWO-8) are shown in Fig. 7(b). The typical trend of the load–displacement history is somewhat similar to the inward loading test except that partial or whole wall collapse occurred at the end of the test (peak system load). The mean masonry cracking load (R_{cr}) was estimated as 1.49 kPa with a COV of 0.22 while the mean veneer system peak (ultimate) load (R_{ul}) was 3.68 kPa with a COV of 0.21. Depending on the collapse load, the deflection capacity of the walls varied significantly across the specimens and the minimum deflection (approx. 30 mm) was recorded for the semi-cyclic loaded specimen. Due to the cyclic nature of the loading, the ties pulled out comparatively easily (low pressure required) from the mortar joint, resulting in lower ultimate deflection and peak pressure of the veneer wall system, despite contrary behaviour being observed for inward semi-cyclic loading. This disparity is due to the nature of the semi-cyclic load, i.e., when ties are in tension with cyclic load, the chance of mortar pull-out of the tie increased significantly. Two distinctive modes of tie failure were observed from the inspection, (i) pull-out of the tie from the mortar joints and (ii) tie connection (nail) pull-out from the timber stud. Veneer cracks as a single horizontal mortar joint and statistically there is an approximately 70% chance of having a horizontal crack at the lower half of the distance between the second and third rows of ties depending on the induced maximum moment and presence of weak mortar joints.

The failure of the veneer wall systems under inward and outward loading is a function of various parameters, mostly bond strength of mortar, tie strength and its failure mechanism, timber stiffness and behaviour of connections between tie-mortar and tie-timber. Hence, the failure mechanism of the veneer wall systems under different directions of loadings (inward and outward) has distinguishing features. Test results involve uncertainties from different laboratory conditions like poor workmanship, bond wrench strength dissimilarities, testing arrangements and loading type. Inward-loading test data has more confidence than outward loading due to the test's complexity involved in the latter case.

3. Stochastic finite element analysis of URM veneer wall system

A three-dimensional (3-D) spatial stochastic finite element model for veneer wall of dimensions 2400 mm (height) × 2400 mm (width) × 110 mm (thickness) was modelled using the commercial software package DIANA FEA 10.3 [35]. A simplified micro-modelling strategy [36] was adopted for the masonry modelling where units are represented by linear elastic continuum elements and the behaviour of the mortar joints, and the unit/mortar interface is lumped into (a zero-thickness interface) discontinuum elements. The individual brick units were modelled elastically as two halves and potential crack planes were modelled with non-linear behaviour using an interface at the mid-length of each brick. On the other hand, mortar joints were modelled using a combined cracking-shearing-crushing model [36,37] which enables the simulation of tensile and shear failure, frictional slip and crushing along the material interfaces. The spatial stochastic FEA includes unit-to-unit (i.e., interface underneath the brick unit to the adjacent interface) spatial variability of flexural tensile bond strength and a spatial correlation of mortar joint $\rho = 0.4$, established by Heffler et al. [38], within courses of masonry, and no correlation (statistical independence) was assumed between masonry courses and

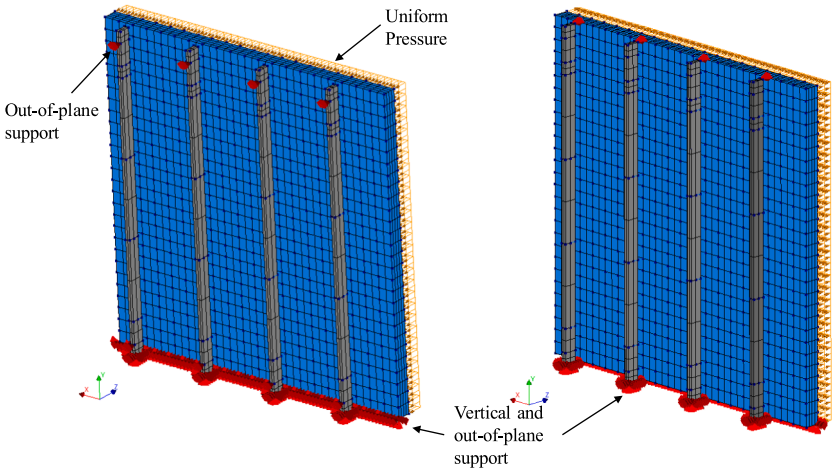

Fig. 8. Finite element model of veneer wall under out-of-plane loading [20].

perpend joints.

The wall ties were modelled as 3-D truss elements with the additional ability to curve. The first row of ties was 300 mm from the bottom of the wall; therefore, four vertical lines of ties (with timber frame) were spaced at 600 mm in the horizontal and vertical direction, as per the tested veneer wall system setup. Each wall tie is side fixed from the masonry wall to timber studs with a 50 mm cavity width. The nonlinear behaviour of the masonry-tie and the tie-timber interfaces were modelled via the wall tie constitutive law, developed from the wall tie characterisation. The veneer wall flexible backup (timber studs) was considered as a 3-D solid element with a linear elastic material in the FEA as no timber studs were cracked (reached beyond the elastic limit) during any of the full-scale veneer wall tests. The timber studs had a cross-section of 90 mm × 35 mm, and the centre-to-centre distance is 600 mm. Material properties were randomly distributed for wall ties and timber stiffness without any consideration of spatial correlation, i.e., statistically independent.

3.1. Loading and boundary conditions

The boundary conditions are consistent with the experimental setup [21] to simulate the testing methodology. To represent the inward (ties are in compression) and outward loading (ties are in tension), uniform pressure loading was applied on the wall's exterior skin in two different directions (see Fig. 8), and the self-weight of the veneer system is also considered. For inward loading, one edge of the first-course units, adjacent to the cavity, was restrained against translation for all directions. Out-of-plane restraint (roller support) was introduced at the top and bottom of the timber studs, at one brick-high distance from the extreme ends, to represent the exact position of the lateral support provided during wall tests. On the other hand, for outward loading, the outer edge (tension side) at the base of the wall was restrained in all directions while the edge adjacent to the cavity is kept free. In addition, the top edge of the timber, closest to the cavity, was supported for lateral out-of-plane direction. Analysis procedures and mesh refinement assessed by Muhit et al. [20] are used in all models. The out-of-plane displacement is recorded at the centre of the unloaded face (height/2, length/2) for each load step and used to establish the load–displacement behaviour of each model.

3.2. Probabilistic material properties

The material properties are categorised as deterministic, spatially variable, and spatially dependent. The flexural tensile strength of the unit-mortar interface is treated as spatially variable, varying along the length and height of the masonry wall, and converted to a direct tensile bond strength value by dividing by a random variable with a mean of 1.5 and COV of 0.13. Cohesion, tensile and compressive fracture energy, and in some cases compressive strength of the masonry are treated as spatially dependent variables, calculated as a function of the direct tensile strength. The remaining material parameters for masonry are considered deterministic based on representative average values as outlined by Muhit et al. [20]. Statistical parameters for flexural tensile strength were selected as obtained from bond strength characterisation (see Table 1). Probabilistic material properties of wall ties were obtained from the probabilistic characterisation of masonry veneer wall ties described in Section 2.2.2 above. DIANA FEA needs as input a stress–strain relationship; hence, the tie-constitutive law (in the form of load–displacement) is converted to the probabilistic stress–strain curve (by dividing the load by cross-sectional area and displacement by unloaded length of the tested tie) and included in the stochastic finite element analysis (SFEA). All the timber studs were modelled as linear elastic in the SFEA; therefore, the elastic modulus is the only variable material property for the timber studs. The reader is referred to Muhit et al. [20] for detailed probabilistic material properties.

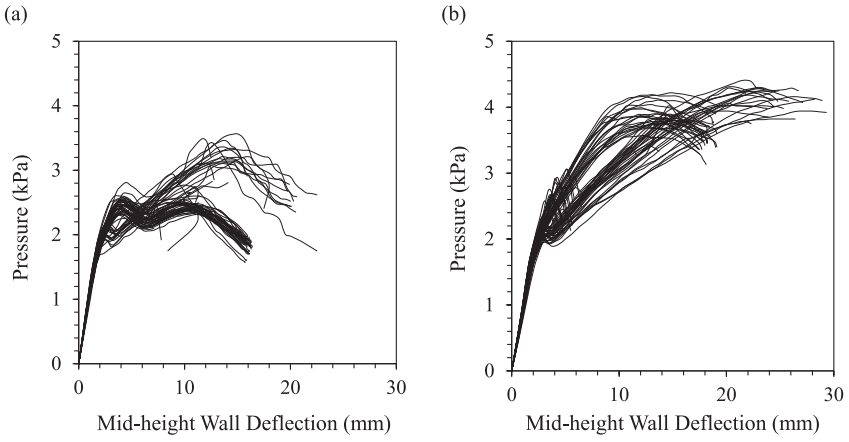

Fig. 9. Pressure load vs deflection plots for MC realisations under (a) inward and (b) outward loading.

3.3. Spatial stochastic FEA results

The deterministic analysis results in system peak load (R_u) as 2.53 kPa and 3.06 kPa for inward and outward loading, respectively. From the SFEA convergence study (as a means of stabilisation of the mean and COV) 60 FE simulations for the inward loading scenario (VWI) and 80 simulations for the outward loading scenario (VWO) were determined as sufficient.

Fig. 9(a) represents the pressure vs mid-height wall deflection outcomes of 60 MCS runs under inward loading and the calculated mean and COV of R_u are 2.71 kPa and 0.13, respectively. Two distinct types of load–displacement behaviour were observed; some of them have a higher second-peak than the veneer cracking load and the remaining are with an equal or lower second peak than the first peak (veneer cracking load). For both types, the cracking pattern depending on the spatial distribution of direct tensile strength at veneer cracking and system peak load is shown and discussed in detail by Muhit et al. [20]. Fig. 9(b) shows the wall deflection plots of 80 MCS runs under outward loading where the mean was 3.55 kPa with a COV of 0.18 for R_u. At the mid-height, the highest crack widths (interface relative displacement) were observed along with some minor cracks along the weaker mortar joints. For both loading scenarios when the distribution of relatively stronger units is much more predominant in the mid-height zone, the veneer cracked at a comparatively higher load. Moreover, as tie strengths were varying spatially for all ties, yielding would occur at different stress levels and the load-sharing mechanism of ties after the veneer cracked governs the ultimate capacity. Moreover, timber stiffness also dictates how timber-tie connections would deflect when pressure load is transferred from the veneer wall to structural backup (timber) via wall ties. The consideration of varying stiffness of the timber studs allows SFEA to incorporate differential deflection. Stiffer timber may accelerate the tie buckling compared to that of more flexible timber by providing 'firmer' lateral support to one line of ties compared to other ties in the same veneer wall specimen.

In order to evaluate the best-fit distributions for each loading case, spatial SFEA is compared to five different distribution types: normal, lognormal, Weibull, Gumbel, and gamma. The Anderson-Darling (A-D) test is applied at the 5% significance level to test the hypothesis that the FEA results are represented by the specified distributions. For all cases, the A-D test failed to reject the null hypothesis for all distributions. The lognormal distribution can be considered the best-fit distribution for both inward and outward loading [25].

A sensitivity analysis study (to evaluate the relative impact of the variability and uncertainty of the SFEA model parameters) was conducted by running the MCS analysis with each parameter in turn modelled deterministically while all other (two) parameters were modelled probabilistically. This study revealed that while the veneer capacity subjected to inward loading is more sensitive to the mortar bond and tie strength than other parameters considered, for outward loading it is only tie strength. Hence only the sensitive parameter(s) can be considered as a variable in the SFEA of the veneer wall system.

3.4. Comparison of MC experimental and SFEA results

A COV obtained from the wall tests may overestimate the true variations of wall failure load (R_u) due to (i) the accuracy of the test measurements and definitions of failure, and (ii) differences between the strengths of the test specimen (full-scale veneer wall systems) and control specimens (e.g., bond-wrench prisms). Therefore, a direct comparison between Monte-Carlo (MC) experimental and SFEA results is not the 'accurate' representation of the FE model's efficiency. Muhit et al. [21] factored out these uncertainties from the experimental COV to make it comparable with SFEA. The comparison summary between Monte-Carlo experimental and spatial SFEA results in terms of the veneer system's peak load is given in Table 3. Spatial SFEA underestimated the R_u experimental mean by 3.2% and 3.5% for inward and outward loading, respectively. Although the COV of SFEA is quite close (0.18) to experimental results (0.19) for the outward loading, for inward loading MC experimental results have a lower COV than SFEA, which is unexpected.

To assess if the test results could be considered part of the same population as the spatial SFEA, Student's *t*-test is conducted. The results indicated that the difference between experimental and SFEA results is not statistically significant, i.e., the SFEA and experimental results can be from the same population for both inward and outward loading categories.

4. Effect of wall tie corrosion

Currently, there are no available standards/codes with design criteria which include the effect of tie corrosion on the ageing masonry structure. Hence the ultimate capacity of the masonry veneer system with corroded ties is unknown and subsequently, there is no framework to investigate the structural reliability. In this study, a framework to include the tie corrosion effect when assessing the veneer capacity and reliability is proposed and compared with the AS 3700 [22] minimum design criteria. As the SFEA (described in Section 3) considered the wall tie as in the new (no corrosion scenario, NCS) condition, to make a reasonable comparison between AS 3700 [22] and SFEA with corroded ties, it is reasonable to modify (reduce) the tie strength in the SFEA to consider the effect of

Table 3
Comparison of experimental and spatial SFEA results of ultimate loads.

Loading Category	Monte-Carlo Experiments		MC Corrected Peak Load (V_E)		Spatial SFEA (V_M)	
	Mean (kPa)	COV	Mean (kPa)	COV	Mean (kPa)	COV
Inward	2.80	0.11	2.80	0.10	2.71	0.13
Outward	3.68	0.21	3.68	0.19	3.55	0.18

corrosion. Therefore, tie strength was assumed to be varied (i.e., uniform distribution) between the measured test value and the AS 3700 design strength value, which is expected to be a lower bound to allow for less-than-perfect workmanship and could also represent ties for which the capacity is reduced by corrosion. As mentioned earlier, in DIANA FEA [35], tie material properties are included as a complete stress–strain relationship, the converted AS 3700 design tie strength (with corrosion effect) would be 43.6 MPa (0.36 kN) and 36.4 MPa (0.30 kN) for compression and tension, respectively for the type of tie used in this study. From the couplet test, mean tie strength was estimated as 126.0 MPa and 160.4 MPa for compression and tension, respectively. When mean tie strength is modified for two data points (compression and tension), it is physically meaningful and necessary to modify the remaining data points of the tie constitutive law (see Fig. 6). Therefore, the mean values for the remaining points in the tie constitutive law are decreased in proportion to the percentage changes in mean peak strength from the couplet test value. Therefore, for each wall, the mean value for the tie constitutive law would be adjusted at the beginning and then based on the statistical parameters (new reduced mean, COV, distribution and correlation) for each point, different stress–strain relationships would be generated for all 20 ties. When mean values of all the data points of the constitutive law were reduced proportionally to include the corrosion effect in the model, the standard deviation was held constant, leading to higher COVs.

4.1. Stochastic FEA results of corrosion scenario

By considering the corrosion scenario (CS), a total of 80 spatial SFEA Monte Carlo simulations (MCS) were completed for each loading direction where convergence for mean and COV were observed, and also to give a sample size sufficient for probabilistic model fitting. Failure was characterised by mid-height cracking, and load–displacement behaviour for inward and outward loading is shown in Fig. 10.

The statistics of peak loading or ultimate resistance (R_u) with corrosion scenario (CS) are shown in Table 4. The mean values of R_u with corrosion scenario (CS) are notably lower than that of no corrosion scenario (NCS) which is expected due to the reduced tie strength input for CS. In contrast, COV for the CS is higher than the NCS type due to the inclusion of additional variability caused by tie corrosion. Similar to NCS, a range of probability distributions were fitted to the spatial SFEA results of CS. Based on the A-D test and CDF^{-1} plot, conservatively lognormal distribution can be considered as the best-fit distribution for both inward and outward loading (see Figs. 11 and 12).

4.2. Model error

The model error (or model uncertainty) of the numerical finite element model used in this study was quantified by Muhit et al. [20] through a comparison of the SFEA results with the experimental peak (failure) loads of URM veneer walls under out-of-plane loading. For inward and outward loading, the mean model error was reported as 1.03 and 1.04, respectively. Conservatively, the COV was estimated as 0.0 for inward loading and 0.06 for outward loading (see Table 4). For simplicity and to establish a closed-form expression, model error statistics can be assumed as lognormally distributed for both inward and outward loading scenarios.

5. Structural reliability analysis

The probability that the load effect exceeds the structural resistance, i.e., probability of failure (p_f) is defined as:

$$p_f = Pr[G(X) \leq 0] = \Pr[R - S \leq 0] = \Phi(-\beta) \tag{1}$$

$$\beta = -\Phi^{-1}(p_f) \tag{2}$$

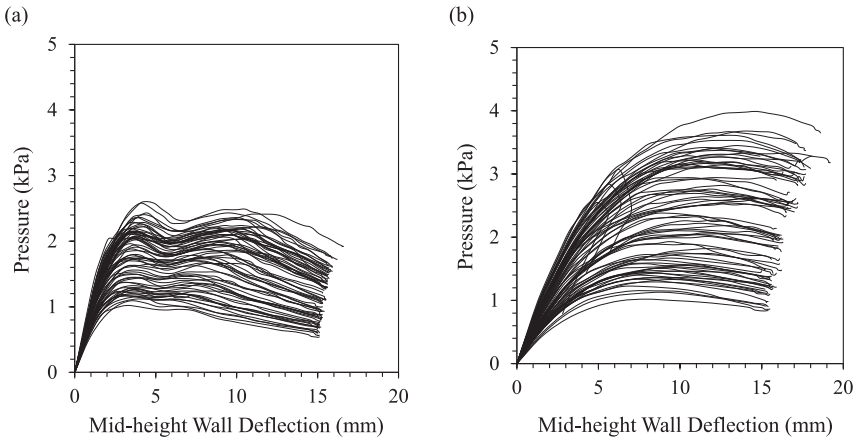

Fig. 10. Pressure-deflection plots for 80 MCS under (a) inward and (b) outward loading considering tie corrosion.

Table 4
Statistical parameters for reliability analysis.

Parameter	Loading	Mean		COV		Distribution	
		NCS	CS	NCS	CS	NCS	CS
Ultimate Resistance, R_u	Inward	2.71 kPa	1.79 kPa	0.13	0.24	Lognormal	Lognormal
	Outward	3.55 kPa	2.39 kPa	0.18	0.34	Lognormal	Lognormal
Model Error, ME*	Inward	1.03		0.0		Lognormal	
	Outward	1.04		0.06		Lognormal	

*source: Muhit et al.[20].

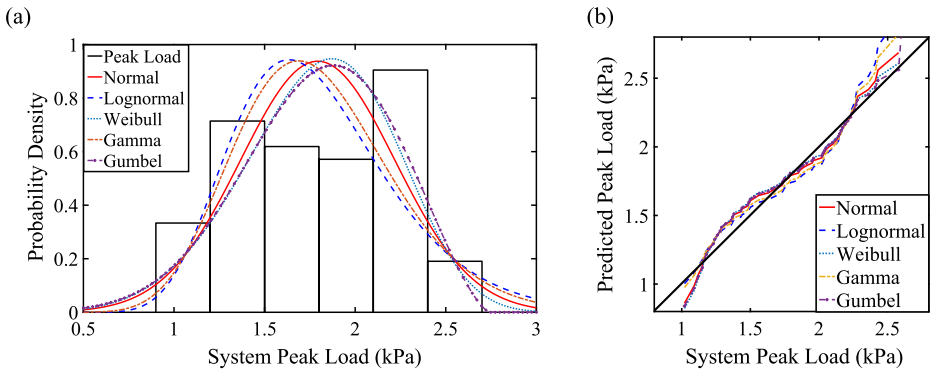

Fig. 11. (a) Probability distribution fits and (b) CDF^{-1} of system peak load for inward loading with CS.

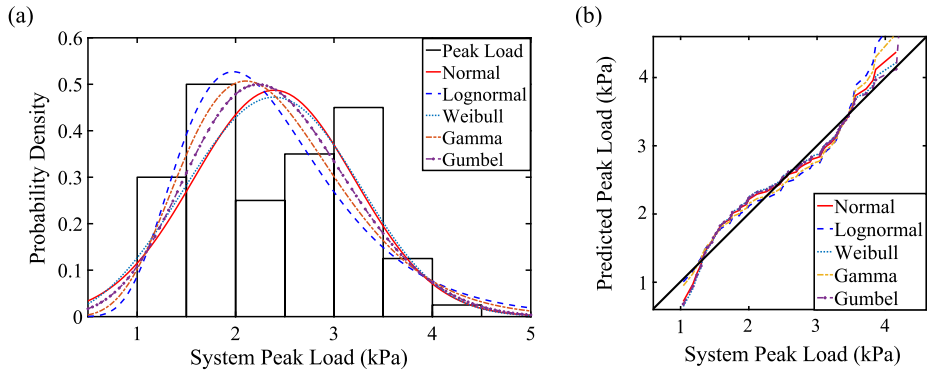

Fig. 12. (a) Probability distribution fits and (b) CDF^{-1} of system peak load for outward loading with CS.

where G(X), the limit state function, describes the performance of the structure in terms of variability factors (X). In the simplest case, R is the resistance of the structure and S is the effect of the applied load actions. Conventionally, $G(X) \leq 0$ denotes the failure of the structure. The reliability index (β) is calculated using the inverse of the standard normal distribution function (Φ^{-1}). In the context of the masonry veneer wall system, the limit state function can be expressed as:

$$G(X) = ME \times R_u - W_p \tag{3}$$

where, ME is the model error, R_u is the resistance determined through spatial SFEA and W_p is the out-of-plane wind loading.

The failure of the masonry veneer wall, i.e., system peak load is governed by the progressive failure of the wall ties. The AS 3700 [22] design limit state for the masonry veneer wall with flexible structural backing can be expressed as $F_{td} \leq \phi F_t$, where ϕ is the capacity reduction factor for wall tie and F_t is the strength of the tie based on its duty rating. According to AS 3700 [22], for the veneer with flexible structural backing, before and after cracking, the design compressive or tensile tie force (F_{td}) shall be taken as 20% of the total tributary lateral load (W_n) (airbag pressure) on a vertical line of ties between horizontal supports. So, F_{td} can be expressed as:

$$F_{td} = 0.2 \times W_n \times H \times d = \phi.F_t \tag{4}$$

Therefore, W_n can be calculated as follows:

$$W_n = \frac{\phi.F_t}{0.2 \times H \times d} \tag{5}$$

where, the distance between two vertical lines of ties (d) is 600 mm, the total height (H) of the wall is 2400 mm, and AS 3700 recommended ϕ is 0.95 for wall ties in tension and/or compression. All the veneer walls tested in the laboratory were constructed with two rows of ties at the top to resist the 2 × F_{td} as per AS 3700. The AS3700 [22] specified tie strength (F_t) for Type A light-duty tie is 0.36 kN and 0.30 kN for compression (inward loading) and tension (outward loading), respectively. The mean-to-nominal statistics for peak annual wind loading for non-cyclonic and cyclonic conditions are based on a recommendation from the Australian Building Codes Board [39], see Table 5.

The wind load statistics are related to nominal resistance as:

$$W_p = W_n\left(\frac{W}{W_n}\right) \tag{6}$$

The probability of failure of the veneer wall can be thus calculated as:

$$p_f = Pr\left[ME \times R_u - W_n\left(\frac{W}{W_n}\right)\right] = Pr\left[ME \times R_u - \frac{\phi.F_t}{0.2 \times H \times d} \times \frac{W}{W_n} \le 0\right] \tag{7}$$

where ME, R_u, and W/W_n are modelled as random variables (see Tables 4 and 5), and all other parameters are deterministic.

5.1. Target reliability

The optimum value of target reliabilities (β_T) is dictated by factors including types of failure, expected costs of failure and costs of increasing existing levels of safety. The type (nature) of the failure is critical in the determination of target reliability, for instance, structural elements that exhibit brittle or sudden failure without pre-warning should be assessed in a higher consequence class. The Australian Standard, AS 5104 [40] (adopted from ISO 2394 [41]), provides a basis for target reliabilities based on a one-year reference period and ultimate limit states for economic (cost-benefit) optimisation (see Table 6).

The present design situation is a single-skin masonry wall with a flexible structural backing subject to a lateral (wind) load – i.e., there is no vertical pre-compression other than the veneer system's self-weight. In this case, the consequence class is minor (expected number of fatalities fewer than 5, smaller buildings and industrial facilities), however, as the failure mode is brittle without pre-warning the consequence class can be increased to Class 3 (moderate consequences of failure – material losses and functionality losses of societal significance, expected number of fatalities fewer than 50, most residential buildings) in Table 6. The Joint Committee on Structural Safety Probabilistic Model Code [42] recommends that the relative cost of safety is medium for 'the most common design situation'. Moreover, consideration of a lower reliability class is recommended in the case of higher uncertainty (coefficient of variation more than 40%). As the COV of peak annual wind load reaches 0.49 (see Table 5), for minor consequences Class 2 and medium relative cost of safety measures the annual target reliability index is $\beta_T = 3.7$. Furthermore, veneer wall systems are mostly for the smaller buildings in Australia; hence, a failure consequence greater than Class 2 is not required.

5.2. Results and discussions

Structural reliability analyses are conducted for a full-sized veneer wall system under inward and outward out-of-plane loading, for cyclonic and non-cyclonic winds. Reliabilities are calculated using a probabilistic model of resistance based on the effect of (a) wall tie corrosion scenario, CS and (ii) no corrosion scenario, NCS. The annual reliabilities are shown in Table 7 for non-cyclonic and cyclonic winds.

In the case of NCS, which considered wall tie connection in a new (non-corroded) condition, the annual reliability (β) well exceeded the target reliability $\beta_T = 3.7$ for both wind classifications (non-cyclonic and cyclonic) and for both loading scenarios (inward and outward loadings). On the other hand, when tie corrosion (CS) is considered, the β index fails to meet the β_T for non-cyclonic regions. Although for outward loading β index exceeded β_T, for inward loading it still fails to meet the target index for cyclonic regions, though not by much. It might appear counter-intuitive that reliabilities are mostly lower for non-cyclonic regions. It does not mean that non-cyclonic wind speeds are higher, but rather indicates that the actual mean wind speeds are proportionally higher than the nominal (design) values for non-cyclonic regions (mean $W/W_n = 0.33$) than they are for cyclonic regions (mean $W/W_n = 0.16$). This is offset, in part, by the significantly higher variability of cyclonic winds.

A reliability-based calibration of AS 3700 [22] is completed considering the target annual reliability index value of 3.7 (class 2) as mentioned earlier that a failure consequence greater than class 2 is not logical for the veneer wall system. The capacity reduction factors determined for non-cyclonic and cyclonic conditions and CS and NCS scenarios are given in Table 8.

For all NCS scenarios, the calculated ϕ factor is more than 1.0 whereas, for a few CS scenarios, a lower ϕ factor is obtained. However, it is important to appreciate that in this study CS scenarios considered the tie corrosion (i.e., lower in strength) for all ties in the veneer system which is indeed over-conservative and represents the lower bound of workmanship. Hence, CS may provide an overly conservative capacity reduction factor estimation. To quantify more realistic ϕ value further studies are needed when only a few of the wall ties have corroded. On the other hand, if the ϕ is equal to 1, it eventually defeats the point of the exercise of having ϕ. However, more future studies are required where F_t can be considered as a variable, unlike this study, to quantify the percentage

Table 5
Statistical parameters W/W_n for peak annual wind loading [39].

Conditions	Mean	COV	Distribution
Non-cyclonic	0.33	0.49	Lognormal
Cyclonic	0.16	0.71	Lognormal

Table 6
Annual target reliabilities (β_T) for economic optimization (adapted from AS 5104, [40]).

Relative Costs of Safety Measures	Consequence of Failure		
	Class 2 (Minor)	Class 3 (Moderate)	Class 4 (Large)
Large	3.1	3.3	3.7
Medium	3.7	4.2	4.4
Small	4.2	4.4	4.7

Table 7
Annual structural reliabilities when $\phi = 0.95$.

Conditions	Annual Reliability Index, β			
	Inward loading		Outward loading	
	NCS	CS	NCS	CS
Non-cyclonic	4.28	3.13	5.02	3.63
Cyclonic	4.42	3.59	5.00	4.02

Table 8
Capacity reduction factor (ϕ) necessary to satisfy target reliability.

Conditions	Capacity reduction factor, ϕ to meet target reliability			
	Inward loading		Outward loading	
	NCS	CS	NCS	CS
Non-cyclonic	>1	0.70	>1	0.91
Cyclonic	>1	0.88	>1	>1

change from AS 3700′s lower bound recommendation.

This proof-of-concept work is preliminary and considered only one particular type (Type-A light-duty) of wall tie. The effect of corrosion indeed, may not be to uniformly reduce all points on the constitutive law established for new ties. However, until such data exists, the approach taken serves to illustrate how the compromised ties may impact the overall veneer wall system behaviour. Moreover, model error statistics are assumed as lognormal distribution; as such collection of additional veneer wall test data is needed to better characterise model errors. In addition, the inclusion of representative bond strength statistics (as in Isfeld et al. [24]), the effect of different wall tie types and then a sensitivity analysis are required to test the robustness of the results. These are areas for further research that will allow for a more robust reliability-based calibration approach to assess the ageing structural component (i.e., veneer wall system) with corroded wall ties or anchorages. Furthermore, a more accurate estimation of the capacity reduction factor (ϕ) considering the various degree of corrosion is needed to assess such ageing structures.

6. Conclusions

The research reported in this paper focused on the experimental and numerical stochastic assessment of URM veneer wall systems (that is, timber as a flexible backup system is connected to masonry wall via metal ties) considering spatial and random variabilities of wall materials under out-of-plane loading. In addition to the estimation of the veneer wall system's failure load, annual structural reliability indices are also calculated considering the corroded and non-corroded wall tie scenarios. The proposed methodology of lowering tie strengths probabilistically can be applied to the estimation of structural resistance or the reliability of historical structures with corroded metal ties and/or anchorages.

Monte-Carlo experimental investigations of 18 full-scale URM veneer wall systems with theoretically identical geometries and properties under out-of-plane loading were conducted. For each loading type, one specimen was tested for semi-cyclic loading while the remaining were tested under monotonic loading. For each batch of mortar mixed, bond wrench testing was conducted at the same age as the test for the associated wall constructed using that mix. A lognormal distribution with an aggregated mean of 0.40 MPa and

0.42 MPa for inward and outward loading, respectively, was estimated for masonry flexural tensile strengths. Parallel to the wall tests, material characterisation tests for masonry were conducted to develop the material model to define the masonry in the nonlinear FEA model. Probabilistic veneer wall tie characterisation is accomplished from 50 brick-tie-timber subassemblies to generate a nonlinear tie constitutive law. After the wall tests, all timber studs used to build the veneer wall were tested to evaluate the modulus of elasticity and bending strength.

A nonlinear spatial stochastic finite element model is developed which considered the spatial variability of the mortar bond strength and random variability of the wall constituent materials to estimate the veneer capacity. From the comparison with experimental results, the stochastic finite element model developed in this study can estimate the behaviour and ultimate load reasonably and is considered to be from the same population as the test results. To include and compare the effect of wall tie corrosion, probabilistic lower tie strengths for all wall ties were considered in the model in addition to new condition (i.e., non-corroded) scenarios. An established method of structural reliability analysis was then applied using the spatial SFEA as a resistance model, considering the random variability of model error and wind load. Annual reliabilities are compared to target reliabilities recommended by AS 5104 (and ISO 2394). Capacity reduction factors and the potential of future studies are discussed while compared to the Australian Masonry Structures Code AS 3700.

As a future research recommendation, full-scale wall tests with weak mortar joints and corroded ties can be accomplished to better understand the historical masonry with steel/iron anchorages; nevertheless, the developed framework could work as a guideline. Further, tie couplet tests can be conducted with a deliberate weak mortar joint to capture the mortar pull-out failure behaviour under tension loading and to buckle inside the mortar joint under compression loading. In addition, similar to the URM veneer wall system, the cavity wall system (another leaf of masonry instead of the flexible backup frame) can be tested under in-plane and out-of-plane loading in order to evaluate the cavity system behaviour. The reliability analysis may incorporate more complex and variable scenarios while the current work is a proof of concept. To further understand the vulnerability and probabilistic behaviour of historical structures under extreme loading other than wind loading, i.e., seismic loads, blast loads, dynamic and impact loads, etc. more studies are recommended.

Declaration of Competing Interest

The authors declare that they have no known competing financial interests or personal relationships that could have appeared to influence the work reported in this paper.

Data availability

Data will be made available on request.

Acknowledgements

The authors acknowledge the financial support of the Australian Research Council under Discovery Project DP180102334.

References

[1] Mendes, F. (2009). Durability of facades [PhD thesis, Universidade do Porto]. Universidade do Porto Research Repository.
[2] BIA, Brick Industry Association (2003). Tech Notes 44b - Wall Ties for Brick Masonry. In: Association, T. B. I. (Ed.) Technical Notes on Brick Construction Reston, Va.
[3] Herald (2017). Newcastle Earthquake: 28 Years After Tragedy Strikes the City. The Herald. 28 December 2017 Ed. Online.
[4] Page, A. W., Kleeman, P. W., Stewart, M. G., & Melchers, R. E. (1990). Structural Aspects of The Newcastle Earthquake. Second National Structural Engineering Conference 1990. Adelaide: Institution of Engineers, Australia.
[5] D. Dowrick, The modified Mercalli earthquake intensity scale - revisions arising from recent studies of New Zealand earthquakes, Bull N Z Soc Earthq Eng 29 (1996) 92–106.
[6] A. Preciado, S.T. Sperbeck, A. Ramírez-Gaytán, Seismic vulnerability enhancement of medieval and masonry bell towers externally prestressed with unbonded smart tendons, Eng. Struct. 122 (2016) 50–61.
[7] Giuffrè, A. (1993). Safety and conservation of historical centers: the Ortigia case. Laterza editor, Rome.
[8] G. Croci, The conservation and structural restoration of architectural heritage, Vol. 1, WIT Press, 1998.
[9] P.B. Lourenço, Recommendations for restoration of ancient buildings and the survival of a masonry chimney, Constr. Build. Mater. 20 (4) (2006) 239–251.
[10] D. Dizhur, X. Jiang, C. Qian, N. Almesfer, J. Ingham, Historical development and observed earthquake performance of unreinforced clay brick masonry cavity walls, SESOC Journal 28 (1) (2015) 55–67.
[11] G. Crevello, N. Hudson, P. Noyce, Corrosion condition evaluations of historic concrete icons, Case Stud. Constr. Mater. 2 (2015) 2–10.
[12] A. Preciado, G. Bartoli, H. Budelmann, The Use of Prestressing Through Time as Seismic Retrofitting of Historical Masonry Constructions: Past, Present and Future Perspective, Ciencia Ergo Sum 22 (3) (2015) 242–252.
[13] ICOMOS (2001). Recommendations for the analysis, conservation and structural restoration of architectural heritage.
[14] Lawrence, S. J. & Lu, J. P. (1991). An elastic analysis of laterally loaded masonry walls with openings. Proceedings of the International Symposium on Computer Methods in Structural Masonry, Swansea, UK.
[15] A.W. Page, J. Kautto, P.W. Kleeman, A Design Procedure for Cavity and Veneer Wall Ties, Masonry International 10 (2) (1996) 55–62.
[16] D. Reneckis, J.M. LaFave, Out-of-plane seismic performance and detailing of Brick Veneer walls, J. Struct. Eng. 136 (7) (2010) 781–793.
[17] A. Preciado, S.T. Sperbeck, Failure analysis and performance of compact and slender carved stone walls under compression and seismic loading by the FEM approach, Eng. Fail. Anal. 96 (2019) 508–524.
[18] D. Foti, Shape Optimization of Rectified Brick Blocks for the Improvement of the out-of-plane Behavior of Masonry, Int. J. Mech. 7 (2013) 417–424.
[19] J. Li, M.J. Masia, M.G. Stewart, S.J. Lawrence, Spatial variability and stochastic strength prediction of unreinforced masonry walls in vertical bending, Eng. Struct. 59 (2014) 787–797.

[20] I.B. Muhit, M.J. Masia, M.G. Stewart, A.C. Isfeld, Spatial Variability and Stochastic Finite Element Model of Unreinforced Masonry Veneer Wall System Under Out-of-plane Loading, Eng. Struct. 267 (2022), 114674.
[21] I.B. Muhit, M.J. Masia, M.G. Stewart, Monte-Carlo laboratory testing of unreinforced masonry veneer wall system under out-of-plane loading, Constr. Build. Mater. 321 (2022), 126334.
[22] AS 3700 (2018). Masonry Structures - AS 3700. Standards Australia Limited, Sydney, Australia.
[23] S.J. Lawrence, M.G. Stewart, Model error and structural reliability for unreinforced masonry walls in vertical bending, Masonry International 24 (1) (2011) 23–30.
[24] A.C. Isfeld, M.G. Stewart, M.J. Masia, Structural Reliability and Partial Safety Factor Assessment of Unreinforced Masonry in Vertical Bending, Australian J. Struct. Eng. (2023), https://doi.org/10.1080/13287982.2023.2173868.
[25] I.B. Muhit, M.G. Stewart, M.J. Masia, Structural Reliability Assessment of Safety Factors for Unreinforced Masonry Veneer Walls Subjected to Out-of-plane Loading. Proceedings of the 14th North American Masonry Conference, 2023.
[26] R.G. Drysdale, A.A. Hamid, Masonry Structures, The Masonry Society, Behavior and Design, 2008.
[27] ASTM Standard A153. (2016). Standard Specification for Zinc Coating (Hot-Dip) on Iron and Steel Hardware - ASTM A153/A153M-16a. ASTM International, West Conshohocken, PA.
[28] Standards Australia/Standards New Zealand. (2003). Masonry units, segmental pavers and flags-Method of test; Method 15: Determining lateral modulus of rupture (AS/NZS 4456.15:2003). Jointly published by Standards Australia International Ltd and Standards New Zealand.
[29] UNI EN. (2002). EN 1052-3. Methods of test for masonry. Part 3: Determination of initial shear strength. Brussels, Belgium.
[30] S.J. Cabardo, T.A.G. Langrish, R. Dickson, B. Joe, Variability in Mechanical and Drying Properties for Blackbutt Timber in New South Wales, J. Inst. Wood Sci. 17 (6) (2007) 311–326.
[31] I.B. Muhit, M.G. Stewart, M.J. Masia, Probabilistic constitutive law for masonry veneer wall ties, Australian J. Struct. Eng. 23 (2) (2022) 97–118.
[32] T.W. Anderson, D.A. Darling, A Test of Goodness-of-fit, J. Am. Stat. Assoc. 49 (268) (1954) 765–769.
[33] Chakravarti, I. M., Laha, R. G., & Roy, J. (1967). Handbook of Methods of Applied Statistics, Volume I, 392-394. New Jersey, United States: John Wiley and Sons.
[34] Standards Australia/Standards New Zealand. (2010). Characterisation of structural timber test methods (AS/NZS 4063.1:2010). Jointly published by Standards Australia International Ltd and Standards New Zealand.
[35] DIANA FEA BV. (2019). DIANA - Finite Element Analysis, User's Manual release 10.3. Delft, The Netherlands.
[36] P.B. Lourenço, J.G. Rots, J. Blaauwendraad, Two approaches for the analysis of masonry structures: micro and macro-modelling, HERON 40 (4) (1995) 313–340.
[37] P.B. Lourenco, J.G. Rots, Multisurface interface model for analysis of masonry structures, J. Eng. Mech. 123 (7) (1997) 660–668.
[38] L.M. Heffler, M.G. Stewart, M.J. Masia, M.R.S. Corrêa, Statistical Analysis and Spatial Correlation of Flexural Bond Strength for Masonry Walls, Masonry Int. J. International Masonry Society 21 (2008) 59–70.
[39] ABCB. (2019). Handbook: Structural Reliability Verification Method. Australian Building Codes Board: Canberra, ACT.
[40] AS 5104. (2017). General principles on reliability for structures. Standards Australia: Sydney, Australia.
[41] ISO 2394. (2015). General Principles on Reliability for Structures. International Organization for Standardization, Geneva.
[42] JCSS. (2021). Probabilistic Model Code: Part I -Basis of Design. 2001. Joint Committee on Structural Safety. https://www.jcss-lc.org/publications/jcsspmc/part_i.pdf [Accessed 10 December 2022].